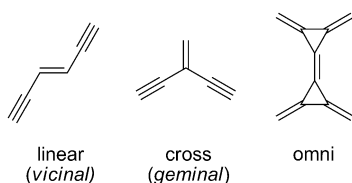


# Conjugation

## Cross-Hyperconjugation: An Unexplored Orbital Interaction between $\pi$ -Conjugated and Saturated Molecular Segments\*\*

Rikard Emanuelsson, Andreas Wallner, Eugene A. M. Ng, Joshua R. Smith, Djawed Nauroozi, Sascha Ott, and Henrik Ottosson\*

$\pi$ -Conjugation, which is the stabilizing interaction between local orbitals of  $\pi$ -symmetry at multiple bonds, is a core concept in chemistry. In the classical sense, a  $\pi$ -conjugated compound has a structure with alternating single and multiple (double and/or triple) bonds.<sup>[1]</sup> However, this model is deceiving in its simplicity because conjugation also depends on the connectivity in the bond alternating path.<sup>[2]</sup> Thus,  $\pi$ -conjugation is divided into linear conjugation (vicinal connectivity), cross-conjugation (geminal connectivity), and



omniconjugation. The first provides a path for delocalization over, for example, a C=C double bond from one end to the other, the second provides strong delocalization paths only from the groups attached to the C=C bond but not between the groups, and the third is a branched system with all parts linearly conjugated.<sup>[3]</sup>

Conjugative interaction is not limited to  $\pi$ -conjugated molecular segments but can also be found in  $\sigma$ -bonded species ( $\sigma$ -conjugation)<sup>[4]</sup> and between  $\sigma$ - and  $\pi$ -systems (hyperconjugation).<sup>[5,6]</sup> Hyperconjugation can further be divided into

1) positive, that is, donation of electron density from filled  $\sigma$ -orbitals to empty  $\pi^*$ -orbitals; 2) negative, that is, interaction between  $\pi$ - or  $p_\pi$ -orbitals with  $\sigma^*$ -orbitals; and 3) neutral hyperconjugation, with no strong directional interaction.<sup>[7]</sup>

The interaction between  $p_\pi$ - or  $\pi$ - and  $\sigma$ -bond orbitals in a linear hyperconjugative connectivity is well-known and often found in charged species.<sup>[8]</sup> However, the fusion of two neutral hyperconjugated paths to a cross-hyperconjugated molecule with geminal connectivity between the two paths should also be considered.<sup>[9]</sup> This interaction would occur in species with two linearly  $\pi$ -conjugated fragments linked by an  $sp^3$  hybridized  $ER_2$  unit ( $E$  = Group 14 element) that contributes with two localized orbitals of  $\pi$ -symmetry; a bonding pseudo- $\pi$  and an antibonding pseudo- $\pi^*$  (Figure 1). These orbitals must be symmetry-adapted combinations of either two  $E-R$   $\sigma$ - or  $\sigma^*$ -bond orbitals, and in the  $C_2$  point group they belong to the  $b$  irreducible representation.

We now report on a study of compounds that are suitable for probing the strength of such potential cross-hyperconjugation. Regular cross-conjugation has recently received increased attention in the fields of nano and materials sciences.<sup>[10,11]</sup> Thus, if strongly cross-hyperconjugated compounds are realizable, they could serve as design alternatives

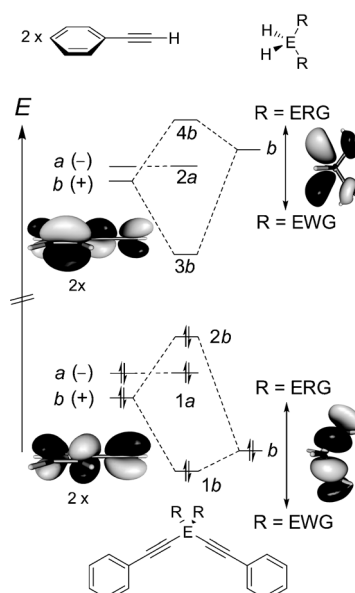


**Figure 1.** Qualitative molecular orbital diagram displaying both the pseudo- $\pi$  and pseudo- $\pi^*$  orbitals ( $b$ -symmetric) of  $H_2ER_2$ , and the in-phase ( $b$ -symmetric) and out-of-phase ( $a$ -symmetric) fragment orbital combinations of the phenylacetylene frontier orbitals (HOMO and LUMO) of the phenylethynyl-phenylethynyl fragment.

[\*] R. Emanuelsson, Dr. A. Wallner, E. A. M. Ng, Dr. H. Ottosson  
Department of Chemistry-BMC, Uppsala University  
Box 576, 75123 Uppsala (Sweden)  
E-mail: henrik.ottosson@kemi.uu.se

Prof. J. R. Smith  
Department of Chemistry, Humboldt State University  
1 Harpst St., Arcata, CA 95521 (USA)

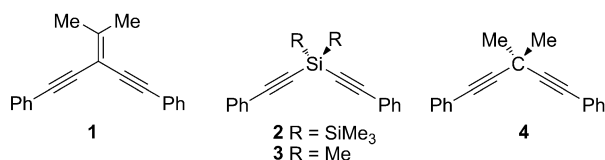
Dr. D. Nauroozi, Dr. S. Ott  
Department of Chemistry-Ångström, Uppsala University  
Box 523, 75120 Uppsala (Sweden)

[\*\*] We are grateful for support from the Swedish Research Council (Grant Nos. 2008-3710, 2009-362, and 2010-4858), Uppsala University through the U3MEC KoF07 initiative, and the Wenner-Gren Foundations, Göran Gustafsson Foundation, and American Scandinavia Foundation for fellowships to A.W. and J.R.S. The National Supercomputer Center (NSC) in Linköping, Sweden, and the Uppsala Multidisciplinary Center for Advanced Computational Science (UPPMAX), Uppsala, Sweden are acknowledged for generous allotment of computer time.

Supporting information for this article is available on the WWW under <http://dx.doi.org/10.1002/anie.201206030>.

to rigid and planar  $\pi$ -conjugated species. Owing to their non-rigid structure they should display higher solubilities than the latter compounds, a fact that can be beneficial from applications point of view. Cross-hyperconjugation would also expand the fundamental understanding of the conjugation phenomenon.

We first investigated bis(phenylethynyl)compounds **1–4**, where **2–4** are substituted at the central Si or C atom. By varying the substituents R from electron-releasing to electron-withdrawing, the energy levels of the pseudo- $\pi$ ( $\text{ER}_2$ ) and pseudo- $\pi^*$ ( $\text{ER}_2$ ) orbitals of the saturated segment are altered and brought closer to the frontier  $\pi$ -orbitals of the phenylethynyl arms (Figure 1). This should afford a varying degree of cross-hyperconjugation as a local filled pseudo- $\pi$ ( $\text{ER}_2$ ) orbital is oriented similarly as a local filled  $\pi$ -bond orbital of a central C=C bond in a cross-conjugated compound. The out-of-phase combination of the pseudo- $\pi$ ( $\text{ER}_2$ ) and the  $b$ -symmetric orbital on the phenylethynyl–phenylethynyl fragment leads to the highest occupied molecular orbital (HOMO) of the assembled molecule. The question then arises as to how extensive this interaction can become.



The heavier Group 14 elements are often found in studies on hyperconjugation, especially in charged species.<sup>[12]</sup> Herein we show that they also provide opportunities for synthetically viable molecules by which the neutral cross-hyperconjugation strength can be varied. The ethynyl segments inserted between the phenyl and  $\text{ER}_2$  groups were incorporated to minimize the steric interaction between the substituents on the E atom and the  $\pi$ -system, and thus, to safe-guard against poor orbital overlap as a result of conformational restrictions that originate from steric congestion.

Initially we set out to match the HOMO energy ( $\epsilon_{\text{HOMO}}$ ) of phenylacetylene with the pseudo- $\pi$ ( $\text{ER}_2$ ) orbitals of various  $\text{H}_2\text{ER}_2$  molecules (in all cases HOMO). Calculations using M062X/6-311G + (2d,p)//B3LYP/6-311G(d) hybrid meta density functional theory (DFT)<sup>[13–16]</sup> reveal that  $\epsilon_{\text{HOMO}}$  of phenylacetylene (−7.96 eV) and 2-methylpropene (−8.25 eV), corresponding to fragments of **1**, differ by less than 0.3 eV (for computational details, see Supporting Information). The pseudo- $\pi$ ( $\text{ER}_2$ ) of  $\text{H}_2\text{Si}(\text{SiMe}_3)_2$  is even closer (−7.98 eV), while the analogous orbitals of  $\text{H}_2\text{SiMe}_2$  (−9.99 eV) and  $\text{H}_2\text{CMe}_2$  (−10.49 eV) are deeper down. With two trifluoromethyl groups at silicon, leading to  $\text{H}_2\text{Si}(\text{CF}_3)_2$ ,  $\epsilon_{\text{HOMO}}$  is −11.58 eV. Thus, bis(trimethylsilyl)bis(phenylethynyl)silane (**2**) should show strong cross-hyperconjugation, and we therefore synthesized **1** and **2**, both reported earlier<sup>[17,18]</sup> (for details see Supporting Information).

The UV absorption spectra of **1** and **2** reveal similar spectral features (Figure 2), with the first absorption should-ers at 298 (**1**) and 281 nm (**2**), respectively, corresponding to

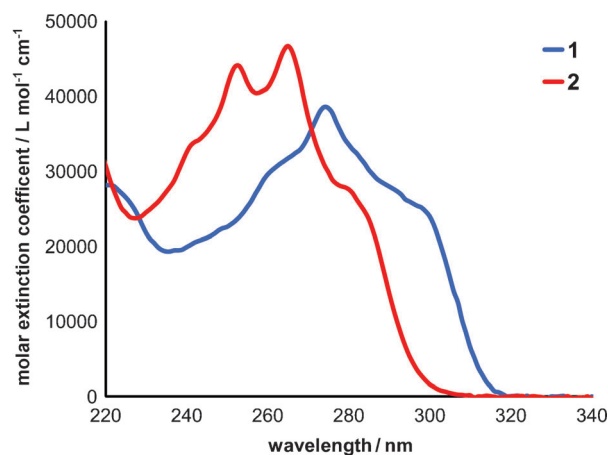
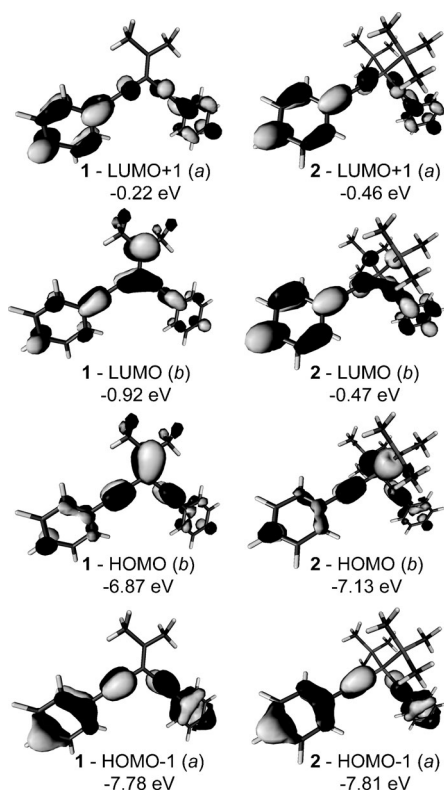


Figure 2. UV absorption spectra of solutions of **1** and **2** in cyclohexane.

excitation energies of 4.17 and 4.42 eV. The second and third absorptions are found at 274 (**1**) and 265 nm (**2**), and at 261 (**1**) and 253 nm (**2**), respectively.

Evaluations of conjugation based on features in UV spectra should however be carried with caution.<sup>[19]</sup> Thus, to further elucidate the similarities the compounds were studied by cyclic voltammetry as well as by DFT calculations, with geometries optimized at B3LYP/6-311G(d) and M062X/6-311G(d) levels and vertical excitations obtained at these geometries by time-dependent DFT (TD-DFT) at TD-M062X/6-311 + G(2d,p) level.<sup>[20]</sup>

The calculations reveal that the analogies persist to the frontier orbitals of **1** and **2**. For example, in the HOMO there is significant orbital density on the  $\text{Si}(\text{SiMe}_3)_2$  moiety of **2** aligned in a cross-conjugated manner, similar as on the  $\text{C}=\text{CMe}_2$  segment of **1** (Figure 3). With regard to orbital energies,  $\epsilon_{\text{HOMO}}$  of **2** is within 0.3 eV from that of **1** (**1**: −6.87, **2**: −7.13 eV). The  $a$ -symmetric HOMO−1 orbitals are nearly isoenergetic (**1**: −7.78, **2**: −7.81 eV) and display strong resemblance which stem from the  $a$  orbital symmetry imposing a nodal plane bisecting the  $\text{ER}_2$  and  $\text{C}=\text{CMe}_2$  moieties. With regard to the lowest and second lowest unoccupied molecular orbitals (LUMO and LUMO + 1), they are clearly analogous in the two compounds, yet in **2** they are isoenergetic but split by 0.70 eV in **1**. The splitting reflects the overlap of the in-phase combination of the LUMO of the phenylethynyl–phenylethynyl fragment with the  $\pi^*(\text{C}=\text{CMe}_2)$  of **1** versus the pseudo- $\pi^*(\text{Si}(\text{SiMe}_3)_2)$  of **2**. It also reflects the distance between the closest two  $\text{sp}^2$ -hybridized C atoms of the phenylethynyl arms (2.412 vs. 2.986 Å in **1** and **2**) and thus the local bonding overlap. This clearly leads to a lower LUMO in **1** than in **2**. With TD-M062X/6-311 + G(2d,p)//B3LYP/6-311G(d) the first transitions in **1** and **2** are 298.9 nm (4.28 eV) and 269.0 nm (4.60 eV), respectively. However, the transitions are to states of opposite symmetries ( $2^1\text{A}$  vs.  $1^1\text{B}$ , Table 1), and this repeats for the second transitions, which are to  $1^1\text{B}$  in **1** and  $2^1\text{A}$  in **2**. Thus, the similarity in the UV absorption spectra of the two compounds is deceiving, as the seemingly analogous transitions involve different excitations.



**Figure 3.** Frontier orbitals of **1** and **2** at the M062X/6-311 + G(2d,p)//B3LYP/6-311G(d) level.

**Table 1:** The first two excitations of **1–4** from UV absorption spectroscopy and the corresponding vertical excitations as calculated with TD-M062X/6-311 + G(2d,p)//B3LYP/6-311G(d).<sup>[a]</sup>

		Transition 1 nm (eV), state sym.	Transition 2 nm (eV), state sym.
<b>1</b>	exp.	298 (4.16)	274 (4.53)
	comp.	289.9 (4.28), 2 <sup>1</sup> A	268.2 (4.62), 1 <sup>1</sup> B
<b>2</b>	exp.	281 (4.41)	265 (4.68)
	comp.	269.0 (4.61), 1 <sup>1</sup> B	265.1 (4.68), 2 <sup>1</sup> A
<b>3</b>	exp.	261 (4.75)	249 (4.98)
	comp.	250.6 (4.95), 1 <sup>1</sup> B	250.1 (4.96), 2 <sup>1</sup> A
<b>4</b>	exp.	253 (4.91)	241 (5.15)
	comp.	241.6 (5.13), 1 <sup>1</sup> B	239.1 (5.18), 2 <sup>1</sup> B

[a] All transitions are visible, with calculated oscillator strengths above 0.20. For **4**, there are four forbidden transitions between the first and second visible excitation.

To determine whether other bis(phenylethynyl)silanes and methanes display similar features as **2**, we synthesized **3** and **4** with ER<sub>2</sub> as SiMe<sub>2</sub> and CMe<sub>2</sub>.<sup>[21]</sup> Compared to **2**, their first UV absorptions are hypsochromically shifted to 261 (**3**) and 253 nm (**4**), respectively, corresponding to raises in energy by 0.34 and 0.49 eV (Figure 4). The TD-M062X calculations reproduce the blue-shift as the first excitation of **4**, a HOMO→LUMO transition leading to the 1<sup>1</sup>B state, is found at 241.6 nm (5.13 eV). However, in **3** the lowest transition is calculated at 250.6 nm (4.95 eV) and it is much more complex. Also, the contribution of the pseudo-π(ER<sub>2</sub>) orbital to the HOMOs of **3** and **4** is negligible, indicating that **3** and **4** are much less cross-hyperconjugated than **2**. Locking

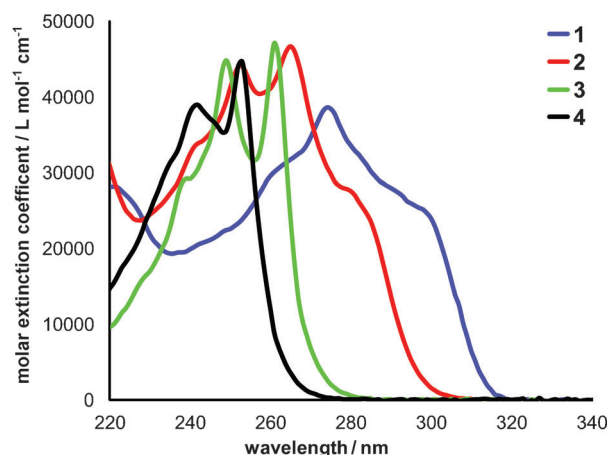


**Figure 4.** UV absorption spectra of solutions of **1–4** in cyclohexane.

the molecules to planar C<sub>2v</sub> symmetric structures so as to optimize the orbital overlap gives more orbital density at the ER<sub>2</sub> segment in **3'** and **4'** (Figure 5), but brings only little change in the calculated first excitation energies.

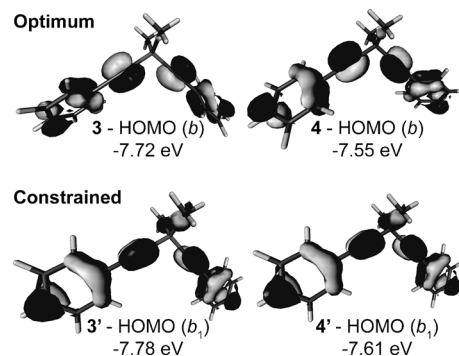


**Figure 5.** The HOMOs of the optimal C<sub>2</sub>-symmetric **3** and **4** and the planar C<sub>2v</sub>-symmetric **3'** and **4'** calculated at the M062X/6-311 + G-(2d,p)//B3LYP/6-311G(d) level.

Further than UV spectroscopy, electrochemically determined redox potentials can provide substantial information on the nature of the frontier orbitals of **1–4**. Thus, the compounds were investigated by means of cyclic voltammetry (CV), and the anodic scans of the CVs of **1**, **2**, **3**, and **4** (Figure 6) feature electrochemically irreversible oxidative processes at 1.17, 1.22, 1.92, and 1.83 V vs. Fc<sup>+</sup>/Fc<sup>0</sup>, respectively. It is thus apparent that compounds **1** and **2** are oxidized at similar potentials, while the oxidations of **3** and **4** are anodically shifted by more than 600 mV. These findings strongly support the results obtained in the UV analysis as well as the DFT calculations in that the HOMOs of **1** and **2** are considerably higher in energy compared to those of **3** and **4**.

The calculated geometries also reveal that **2** is more related to **1** than is **3** and **4**, as the C2-C1-C1'-C2' dihedral angle  $\theta$  involving the inner *ortho*- and the *ipso*-C atoms of the phenyl groups (Table 2), which measures the out-of-plane rotation of the phenyl groups and thus reflects the linear  $\pi$ -

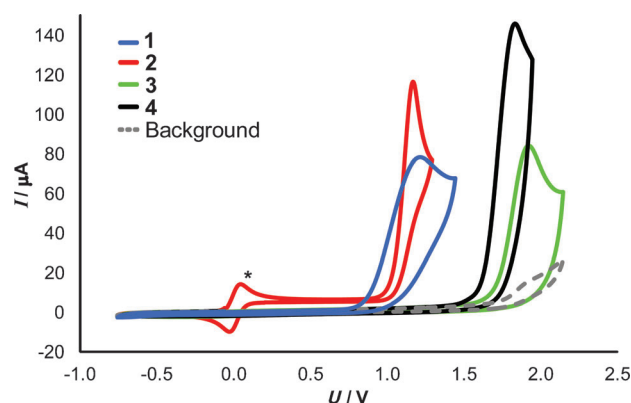


**Figure 6.** Cyclic voltammograms (anodic scans) of **1–4** (1 mM solutions in CH<sub>3</sub>CN) containing 0.1 M NBu<sub>4</sub>PF<sub>6</sub> versus Fc<sup>+</sup>/Fc<sup>0</sup>,  $\nu = 100 \text{ mV s}^{-1}$ . \* Fc<sup>+</sup>/Fc<sup>0</sup> couple as internal standard.

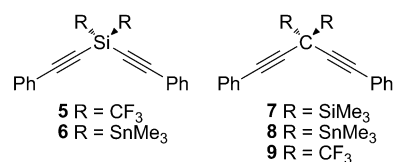
**Table 2:** Dihedral angle  $\theta$  and essential CC bond lengths calculated at B3LYP/6-311G(d) (normal) and M062X/6-311G(d) (*italics*) levels.<sup>[a]</sup>

Molecule, sym.		$\theta$ [°]	$r_{\text{C}=\text{C}}$ [Å]	$r_{\text{C}-\text{C}(\text{Ph})}$ [Å]	$\Delta r_{\text{cc}}(\text{Ph})$ [Å]
1	C <sub>2</sub>	10.7	1.210	1.423	1.394–1.407
2	C <sub>2</sub>	49.6	1.218	1.425	1.390–1.406
	C <sub>1</sub>	44.6	1.213/1.213	1.431/1.431	1.388–1.400
3	C <sub>2</sub>	89.3	1.215	1.426	1.390–1.406
4	C <sub>2</sub>	84.5	1.208	1.428	1.390–1.406
5	C <sub>2</sub>	49.7	1.214	1.423	1.389–1.406
6	C <sub>2</sub>	0.0	1.230	1.433	1.399–1.414
	C <sub>1</sub>	0.0	1.226/1.226	1.438/1.438	1.395–1.406
7	C <sub>2</sub>	8.2	1.210	1.426	1.390–1.407
	C <sub>1</sub>	8.2	1.210	1.427	1.390–1.407
8	C <sub>2</sub>	0.0	1.226	1.433	1.399–1.415
	C <sub>1</sub>	2.3	1.223/1.223	1.437/1.437	1.395–1.408
9	C <sub>2</sub>	54.2	1.203	1.426	1.390–1.405

[a]  $\theta$  denotes the C2-C1-C1'-C2' dihedral angle involving the inner *ortho*- and the *ipso*-C atoms of the phenyl groups,  $\Delta r_{\text{CC}}(\text{Ph})$  denotes the C–C bond length range of the Ph groups. Here, only values of species with bulky R = SiMe<sub>3</sub> or SnMe<sub>3</sub> are given with both B3LYP and M062X; for the full table see the Supporting Information.

conjugation/hyperconjugation strengths between the phenylethynyl arms and either the C=CMe<sub>2</sub> or ER<sub>2</sub> segments, has values with B3LYP of 10.7° (**1**), 49.6° (**2**), 89.3° (**3**), and 84.5° (**4**), respectively. Interestingly, the dihedral angle of **2** is even smaller with M062X, a dispersion corrected DFT method suitable to handle steric congestion such as between the two SiMe<sub>3</sub> groups of **2**. On the other hand, no significant differences are seen in analogous CC bond distances of these compounds, even not when comparing the regularly cross-conjugated **1** with **3** and **4** (Table 2). The same holds for experimentally determined NMR chemical shifts, as there are no significant differences in the aromatic region of **1** when compared to those of **2–4**.

We also computed how cross-hyperconjugation varies with atom E and a wider set of substituents R. For E = Si, a span in the excitation energies is provided by R = CF<sub>3</sub> (**5**) and SnMe<sub>3</sub> (**6**) giving a wavelength (energy) range for the first visible excitation of 249.6–276.3 nm (4.49–4.97 eV). Here, compound **6** was calculated at TD-M062X/LANL2DZdp//B3LYP/LANL2DZdp level,<sup>[22]</sup> and the first excitation of **2** at



this level is 270.4 nm (4.58 eV). With E as C and R as either SiMe<sub>3</sub> (**7**), SnMe<sub>3</sub> (**8**), or CF<sub>3</sub> (**9**) excitations at 264.3 nm (4.69 eV), 286.5 nm (4.33 eV), and 235.0 nm (5.28 eV) are found. Thus, the computations reveal possibilities for wider tuning of the first transition when E = C than when E = Si, and compound **8** is the best cross-hyperconjugated analogue of **1**. Yet, an important difference between **1** and the cross-hyperconjugated species, excluding **6**,<sup>[23]</sup> is that the first transition in **1** is to the 2<sup>1</sup>A state, whereas in **2–5** and **7–9** it is to the 1<sup>1</sup>B state.

A striking geometry feature of **6–8** is that these species are either planar C<sub>2v</sub>-symmetric (**6** and **8**, Table 2), or nearly so (**7**), supporting strong cross-hyperconjugation. It is also notable that the C≡C triple bonds in **6** and **8** are notably elongated when compared to **1**. From the calculated lowest excitation energies and the geometries, it is thus apparent that cross-hyperconjugation strength can be tuned through choice of element E and substituents R, in a similar manner as found earlier for the hyperconjugative donor and acceptor abilities of C–X σ-bonds.<sup>[24]</sup> In our species, electropositive R groups raise the energy of the pseudo-π(ER<sub>2</sub>) orbital as well as polarize the E–R σ-bond electron density towards the E atom.

In conclusion, through a series of easily accessible and persistent compounds we have shown that a properly substituted ER<sub>2</sub> segment has similar effect on the electronic and optical properties of a molecule when inserted between two linearly π-conjugated segments as a C=C double bond with geminal connectivity. This cross-hyperconjugation provides new design motifs for compounds with applications in nano and materials sciences. A next question is now whether omnihyperconjugated molecules can also be designed.

Received: July 27, 2012

Revised: September 26, 2012

Published online: November 26, 2012

**Keywords:** conjugation · cross-conjugation · Group 14 elements · hyperconjugation · optical tuning

- [1] R. Hoffmann, C. Janiak, C. Kollmar, *Macromolecules* **1991**, *24*, 3725–3746.
- [2] M. Bruschi, M. G. Giuffreda, H. P. Lüthi, *Chem. Eur. J.* **2002**, *8*, 4216–4227.
- [3] Linear conjugation: H. Wang, R. Helgeson, B. Ma, F. Wudl, *J. Org. Chem.* **2000**, *65*, 5862–5867; Cross-conjugation: N. F. Phelan, M. Orchin, *J. Chem. Educ.* **1968**, *45*, 633–637; M. Trättelberg, H. Hopf, *Acta Chem. Scand.* **1994**, *48*, 989–993; Omniconjugation: M. H. van der Veen, M. T. Rispens, H. T. Jonkman, J. C. Hummelen, *Adv. Funct. Mater.* **2004**, *14*, 215–223.
- [4] R. D. Miller, J. Michl, *Chem. Rev.* **1989**, *89*, 1359–1410.



- [5] a) R. S. Mulliken, *J. Chem. Phys.* **1939**, *7*, 339–352; b) R. S. Mulliken, C. A. Rieke, W. G. Brown, *J. Am. Chem. Soc.* **1941**, *63*, 41–56.
- [6] For thorough reviews on  $\pi$ - and  $\sigma$ -delocalization, see *Chem. Rev.* **2005**, *105*, all of issue 10.
- [7] For a recent review of hyperconjugation, see: I. V. Alabugin, K. M. Gimore, P. W. Peterson, *WIREs Comput. Mol. Sci.* **2011**, *1*, 109–141.
- [8] a) N. Muller, R. S. Mulliken, *J. Am. Chem. Soc.* **1958**, *80*, 3489–3497; b) P. v. R. Schleyer, A. J. Kos, *Tetrahedron* **1983**, *39*, 1141–1150; c) R. Hoffmann, *J. Chem. Phys.* **1964**, *40*, 2480–2488.
- [9] We use the term cross-hyperconjugation instead of hypercross-conjugation to stress that the geminal connectivity of the conjugated paths should have higher priority than the specific conjugation type.
- [10] a) M. Gholami, R. R. Tykwinski, *Chem. Rev.* **2006**, *106*, 4997–5027; b) P. A. Limacher, H. P. Lüthi, *WIREs Comput. Mol. Sci.* **2011**, *1*, 477–486; c) H. Hopf, M. S. Sherburn, *Angew. Chem.* **2012**, *124*, 2346–2389; *Angew. Chem. Int. Ed.* **2012**, *51*, 2298–2338.
- [11] a) G. C. Solomon, D. Q. Andrews, R. P. Van Duyne, M. A. Ratner, *J. Am. Chem. Soc.* **2008**, *130*, 7788–7789; b) G. C. Solomon, D. Q. Andrews, R. H. Goldsmith, T. Hansen, M. R. Wasielewski, R. P. Van Duyne, M. A. Ratner, *J. Am. Chem. Soc.* **2008**, *130*, 17301–17308; c) G. C. Solomon, D. Q. Andrews, R. P. Van Duyne, M. A. Ratner, *ChemPhysChem* **2009**, *10*, 257–264; d) A. B. Ricks, G. C. Solomon, M. T. Colvin, A. M. Scott, K. Chen, M. A. Ratner, M. R. Wasielewski, *J. Am. Chem. Soc.* **2010**, *132*, 15427–15434.
- [12] a) J. B. Lambert, C. E. Shawl, E. Basso, *Can. J. Chem.* **2000**, *78*, 1441–1444; b) J. B. Lambert, Y. Zhao, R. W. Emblidge, L. A. Salvador, X. Liu, J.-H. So, E. C. Chelius, *Acc. Chem. Res.* **1999**, *32*, 183–190; c) J. B. Lambert, G. T. Wang, R. B. Finzel, D. H. Teramura, *J. Am. Chem. Soc.* **1987**, *109*, 7838–7845; d) J. B. Lambert, *Tetrahedron* **1990**, *46*, 2677–2689; e) J. B. Lambert, G. T. Wang, D. H. Teramura, *J. Org. Chem.* **1988**, *53*, 5422–5428; f) J. B. Lambert, R. A. Singer, *J. Am. Chem. Soc.* **1992**, *114*, 10246–10248; g) M. A. Cook, C. Eaborn, D. R. M. Walton, *J. Organomet. Chem.* **1970**, *24*, 293–299; h) U. Weidner, A. Schweig, *Angew. Chem.* **1972**, *84*, 550; *Angew. Chem. Int. Ed.* **1972**, *11*, 536–537.
- [13] Gaussian09 (Revision A.1). Frisch, M. J. et al. Gaussian, Inc., Wallingford CT, **2009**. For the complete reference, see the Supporting Information.
- [14] a) A. D. Becke, *J. Chem. Phys.* **1993**, *98*, 5648–5652; b) P. J. Stevens, F. J. Devlin, C. F. Chablowski, M. J. Frisch, *J. Phys. Chem.* **1994**, *80*, 11623–11627.
- [15] a) R. Krishnan, J. S. Binkley, R. Seeger, J. A. Pople, *J. Chem. Phys.* **1980**, *72*, 650–654; b) A. D. McLean, G. S. Chandler, *J. Chem. Phys.* **1980**, *72*, 5639–5648.
- [16] a) Y. Zhao, D. G. Truhlar, *Theor. Chem. Acc.* **2008**, *120*, 215–241; b) Y. Zhao, D. G. Truhlar, *J. Chem. Theory Comput.* **2008**, *4*, 1849–1968.
- [17] W. Yan, X. Ye, N. G. Akhmedov, J. L. Petersen, X. Shi, *Org. Lett.* **2012**, *14*, 2358–2361.
- [18] C. Mechtler, M. Zirngast, J. Baumgartner, C. Marschner, *Eur. J. Inorg. Chem.* **2004**, 3254–3261.
- [19] a) M. Klokkenburg, M. Lutz, A. L. Spek, J. H. van der Maas, C. A. van Walree, *Chem. Eur. J.* **2003**, *9*, 3544–3554; b) N. N. P. Moonen, F. Diederich, *Org. Biomol. Chem.* **2004**, *2*, 2263–2266.
- [20] a) E. Runge, E. K. U. Gross, *Phys. Rev. Lett.* **1984**, *52*, 997–1000; b) D. Jacquemin, E. A. Perpète, I. Ciofini, C. Adamo, *J. Chem. Theory Comput.* **2010**, *6*, 1532–1537.
- [21] H. E. Zimmerman, J. A. Pincock, *J. Am. Chem. Soc.* **1973**, *95*, 3246–3250.
- [22] a) W. R. Wadt, P. J. J. Hay, *Chem. Phys.* **1985**, *82*, 284–298; b) C. E. Check, T. O. Faust, J. M. Bailey, B. J. Wright, T. M. Gilbert, L. S. Sunderlin, *J. Phys. Chem. A* **2001**, *105*, 8111–8116.
- [23] Compound **6** is analogous to **1**, with the first transition to the  $2^1A$  state and the second to the  $1^1B$  state.
- [24] a) I. V. Alabugin, T. A. Zeidan, *J. Am. Chem. Soc.* **2002**, *124*, 3175–3185; b) I. V. Alabugin, M. Manoharan, *J. Org. Chem.* **2004**, *69*, 9011–9024.